Light propagation in optically induced Fibonacci lattices

Martin Boguslawski^{1,*}, Nemanja M. Lučić², Dejan V. Timotijević², Cornelia Denz¹, and Dragana M. Jović Savić²

¹Institut für Angewandte Physik and Center for Nonlinear Science (CeNoS), Westfälische Wilhelms-Universität Münster, 48149 Münster, Germany

² Institute of Physics, University of Belgrade, P.O. Box 68, 11001 Belgrade, Serbia

*Corresponding author: martin.boguslawski@uni-muenster.de

We report on the optical induction of Fibonacci lattices in photorefractive strontium barium niobate by use of Bessel beam waveguide-wise writing techniques. Fibonacci elements \mathcal{A} and \mathcal{B} are used as lattice periods. We further use the induced structures to execute probing experiments with variously focused Gaussian beams in order to observe light confinement owing to the quasiperiodic character of Fibonacci word sequences. Essentially, we show that Gaussian beam expansion is just slowed down in Fibonacci lattices, as compared with appropriate periodic lattices.

1 Introduction

Irregular lattices are of high interest as they break the scheme of Bloch wave propagation in contrast to periodic arrangements, but still allow for introducing proper quasi band gaps where propagation is forbidden. It was during the 1980s that quasiperiodic structures in solid state physics amazed the scientific community [1] as it was not clear until then that structures holding short range but lacking long range order [2] can emerge in nature. As in many cases solid state physics can easily be transferred to photonic systems since their mathematical description of wave propagation have similar structures, only a short time after this discovery first optical experiments were implemented in order to analyze quasiperiodic media [3–5]. Such as in the latter publication, asking for quasiperiodic structures rapidly the nomenclature of a Fibonacci grating came up for this often is referred to as the embodyment of irregularity [2,6]. Since then, numerous experiments and theoretical considerations were realized in order to discover the secrets of aperiodic and quasiperiodic media in more detail exploiting the example of Fibonacci structures [7–10]. From the industrial and applicational point of view, it came during the last years that quasi-, aperiodic and disordered structures are of particular interest for solar cell manufacturing as light in a cell with these structurings can be forced to follow a longer path inside the absorbing medium as in unstructured or periodic realizations [5, 11, 12].

It was recently presented that the optical induction technique can be extended in terms of allowing for waveguide-wise writing of desired binary structures [13, 14]. Using multiple induction beams of narrow power confinement at least in two dimensions accordingly bears the opportunity to have a closer look at quasi- and aperiodic structures, as in contrast the one-beam methods to induce irregular structures are inherently limited. The reason is, these structures show a radially wide spread power spectrum which is in conflict with the noteworthy and sufficient criterion of a circle-like writing beam spectrum. Such a spectrum is necessary in order to generate so-called (2+1)-dimensional structures, where the refractive index is modulated in the two transverse directions but keeps constant along the third dimension. This dimensionality excellently allows to model a temporal development of a 2d wave system as the unmodulated direction can be identified with the time dimension. Various model systems were designed in the past basing on such a scheme, ranging from Bloch oscillation, Zener tunneling, Anderson localization, as well as coherent backscattering. Of further particular interest is the nonlinear response of the chosen photorefractive medium, accordingly, various soliton formations were investigated, such as bulk, discrete and vortex solitons.

2 Quasiperiodic Fibonacci lattice

Our approach to design a quasiperiodic Fibonacci pattern is to vary the distance of adjacent waveguides in terms of Fibonacci words. Thereby we select two different Fibonacci sequences for two orthogonal directions, were one Fibonacci sequence is part of a Fibonacci word. Fibonacci words are binary sequences where, according to the Fibonacci series, the nth word is generated by putting together the (n-1)st and the (n-2)nd word, such as

$$\mathcal{S}_n = \{ \mathcal{S}_{n-1} \mathcal{S}_{n-2} \}. \tag{1}$$

Giving the first two words determines the complete set of all words. We define two different distances \mathcal{A} and $\mathcal{B} = \mathcal{A}/\varphi$ where $\varphi = (1 + \sqrt{5})/2$ is the golden ratio, and set $\mathcal{S}_0 = \mathcal{A}$ and $\mathcal{S}_1 = \mathcal{A}\mathcal{B}$ such that the first 5 Fibonacci words read as

$$S_0 = A,$$
 $S_1 = AB,$
 $S_2 = ABA,$
 $S_3 = ABAAB,$
 $S_4 = ABAABABA.$
(2)

Picking two subwords u of length N from a very long Fibonacci word S_n with $n \gg N$ starting with arbitrary but for both orthogonal directions various elements, we receive an quasiperiodic, non-symmetric structure of $N \times N$ sites as depicted in Fig. 1(a). You can find here, that the typical character of a Fibonacci word can be found in every direction. That is, distance A is more probable than B, as the probability for A is 0.62, and this bears typical structure groups: quad, double and single waveguide elements.

3 Experimental techniques

After we have determined the waveguide positioning scheme, we can apply an incoherent-Bessel beam induction method which is writing every single waveguide with an appropriate nondiffracting Bessel beam of zeroth order.

In general, our experimental setup is appropriate to generate any kind of nondiffracting beam by usage of a set of spatial light modulators (SLM) [15]. The corresponding scheme is presented in Fig. 2 and the induction process is analogous to Ref. [13]. That is, the usage of SLMs allows us to realize numerically calculated light fields in a particular image plane defined by the choice of a set of lenses including a demagnification factor of roughly 1/6. Particularly, the PSLM is positioned in real space in order to modulate incoming plane waves accordingly. Low-pass filtering spatial spectra in Fourier space can be achieved by the ASLM that therefore converts computer generated binary circular masks to corresponding blocking filters.

For the induction, we are dealing with Bessel beams belonging to the group of nondiffracting beams. Therefore, there exists a finite volume where the transverse intensity distribution is almost constant along a particular distance in direction of propagation. This distance is closely connected to the diameter of every contributing partial light field, i.e. determined by the area of the SLM, and the demagnification factor. Moreover, a further crucial factor for this length is the structural size g.

In contrast to higher order Bessel beams with zero intensity in the central area, Bessel beams of zeroth order have a distinguished intensity maximum here. To resemble the desired Fibonacci structure, we basically need to change the position of a writing beam to bring the central maximum to the defined lattice positions given by the designed structure. Consequently, for implementing a 9×9 structure as presented in Fig. 1(a), we have 81 various positions given. Changing transversely the beam position can be done easily as computationally a sparse matrix with the necessary position information included needs to be convoluted with a basic Bessel beam light field distribution that in turn needs to be calculated only once.

Optical induction into the SBN crystal then occurs at an externally applied field of 1000 V. During the induction process, it is necessary to give the information of each single Bessel beam sequentially to the SLM in order to generate a corresponding light field in the volume of interest. The reason therefor is obvious, as a coherent overlap of all contributing Bessel beams would end up in an incorrect intensity distribution as mixed terms of the field summation of all 81 fields would contribute additionally. However, introducing an effective intensity I_{eff} , we aim to implement the summation of all intensities $I_{\text{eff}} = \sum_{\mathbf{k}} I_{\mathbf{k}} = \sum_{\mathbf{k}} |E_{\mathbf{k}}|^2$ rather than the absolute square of all light fields $I = |\sum_{\mathbf{k}} E_{\mathbf{k}}|^2$. This implies to utilize an inhomogeneous approach such as multiplexing induction schemes. Simulated and experimentally determined effective intensities are given in Fig. 1(b) and (c). Intensity distributions of writing and probing

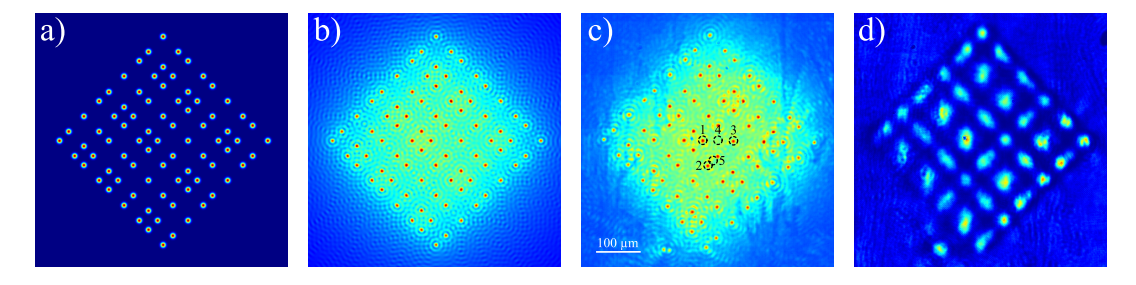


Figure 1. In (a) basis Fibonacci lattice is presented with Gaussian envelopes at every lattice site. (b): Simulated effective Bessel beam intensity with appropriate structural size forming desired Fibonacci lattice. (c): Measured effective intensity taken by multiple-shot illumination at backface of crystal, dashed circles denote considered Gaussian probe beam input positions. (d): Experimental plane probing wave output at exit face of crystal.

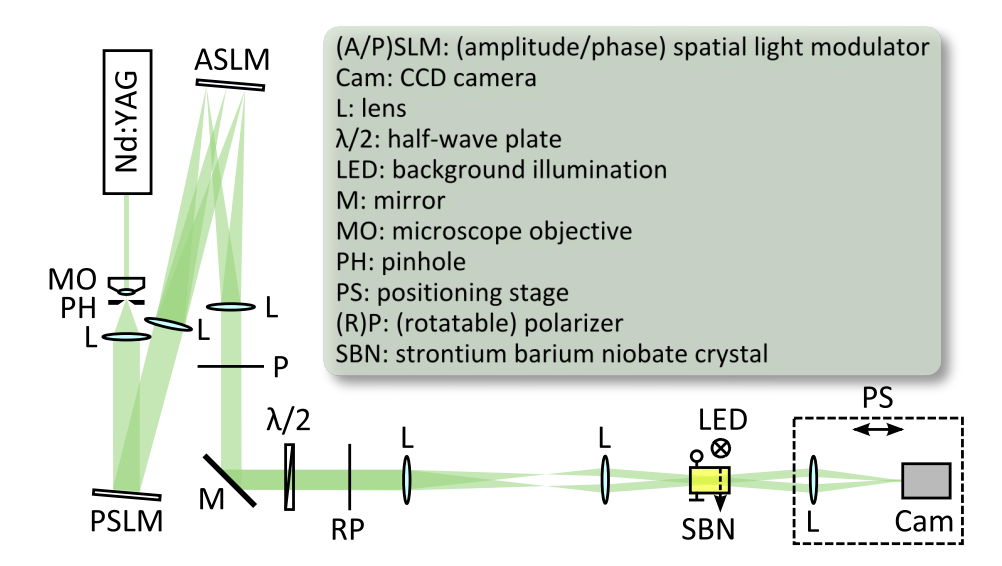


Figure 2. Experimental setup for induction of Fibonacci lattice by Bessel multiplexing technique.

light fields are recorded by a CCD camera imaging system that is mounted on a positioning stage in order to shift the corresponding image plane to the exit face of the crystal. A LED is implemented above the crystal to erase the inscribed structure in order to induce further light potentials.

For an actual implementation, we need to settle the structural size g of the Bessel beam intensity as the diameter of the inner maximum scales proportionally with g in order to determine the waveguide diameter. In detail, we fix g to $14\,\mu\mathrm{m}$ and \mathcal{A} to $42\,\mu\mathrm{m}$, where \mathcal{B} is then determined to $26\,\mu\mathrm{m}$. This yields an effective waveguide distance of $32\,\mu\mathrm{m}$ given by the statistics of a Fibonacci word \mathcal{S} .

Figure 1(d) shows the output intensity after probing the structure with a plane wave. Notice, that waveguide positions of quad and double elements cannot be separated with this waveguide analysis method as the particular configuration of perpendicular probing incidence produces these confined intensity bunches. However, we will see later on that single waveguide stimulation is possible with a properly focused Gaussian beam and that waveguide clusters are induced accurately according to the effective intensity distribution.

4 Light propagation characteristics in Fibonacci photonic lattice: Experiment vs. numerics

Next, we investigate the influence of optically induced Fibonacci photonic lattices on the beam propagation and localization in the linear regime, that is, at low probing beam power of several μ W. In order to theoretically model light propagation in quasiperiodic Fibonacci photonic lattices along the propagation direction z, we consider paraxial wave equation for the slowly varying electric field amplitude $A(\vec{r})$:

$$\left\{2ik\frac{\partial}{\partial z} + \Delta_{\perp} - kn_{\rm e}^2 r_{33} \left(\frac{\partial}{\partial x} \Phi_{\rm sc}\right)\right\} A(\vec{r}) = 0.$$
 (3)

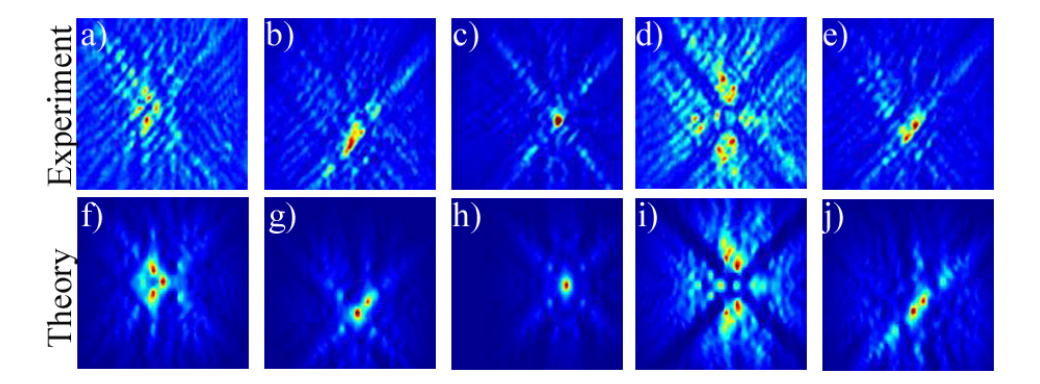


Figure 3. Light propagation in quasiperiodic Fibonacci photonic lattice. Intensity beam distributions at the exit face of crystal experimentally observed (first row), and numerically calculated (second row), for input probe beam size 6 μm. Columns correspond to input beam positions 1,2,3,4 and 5 (from Fig. 1(c)) respectively.

In this equation, k is the wave number, Δ_{\perp} the divergency in transverse direction perpendicular to z, $n_{\rm e}$ extraordinary refractive index coefficient, r_{33} the corresponding electro-optical coefficient for extraordinary polarization and $\Phi_{\rm sc}$ describes the potential of the internal electric field. For solving our model equation we use the split-step method with the parameters of our experiment.

A probe beam is launched at different incident positions as marked in Fig. 1(c) and, accordingly, beam propagation in Fibonacci photonic lattices fabricated in our crystal is studied. Figure 3 presents typical results of light propagation characteristics inside a Fibonacci photonic lattice with respect to the different incident positions, observed both experimentally and numerically.

We choose few typical incident positions at the lattice sites, or between them, marked by numbers 1, 2, 3, 4 and 5 in Fig. 1(c). These positions correspond to results in the first, second, third, fourth and fifth column in Fig. 3, respectively. The first row presents typical intensity distributions at the exit face of the crystal observed experimentally while the second row represents the corresponding distributions obtained numerically. A very good qualitative agreement between these two sets of obtained intensity profiles can be observed. The propagating beam in the lattice is subjected to different competing influences: broad in the linear media, filament in the lattice sites, focuses in some sites and have a tendency to localization. One can see better localization for incident positions 2 and 3 at the lattice sites (second and third column) and position 5 between sites (fifth column). A very strong influence on the localization process has the separation between incident and neighboring lattice sites.

5 Comparison with beam propagation in periodic lattice

We study numerically the beam propagation in Fibonacci photonic lattice considering propagation behavior along the propagation distances ($L=15\,\mathrm{mm}$). In such kind of deterministic systems (as well as in disordered) it is usual to perform analysis with averaging over different input beam positions, in order to remove effects of the local environment, i.e. the influence of the neighboring waveguides. For quantitative analysis we use a relevant quantity for the characterization of the localization level, the effective beam width $\omega_{\mathrm{eff}}=P^{-1/2}$, where

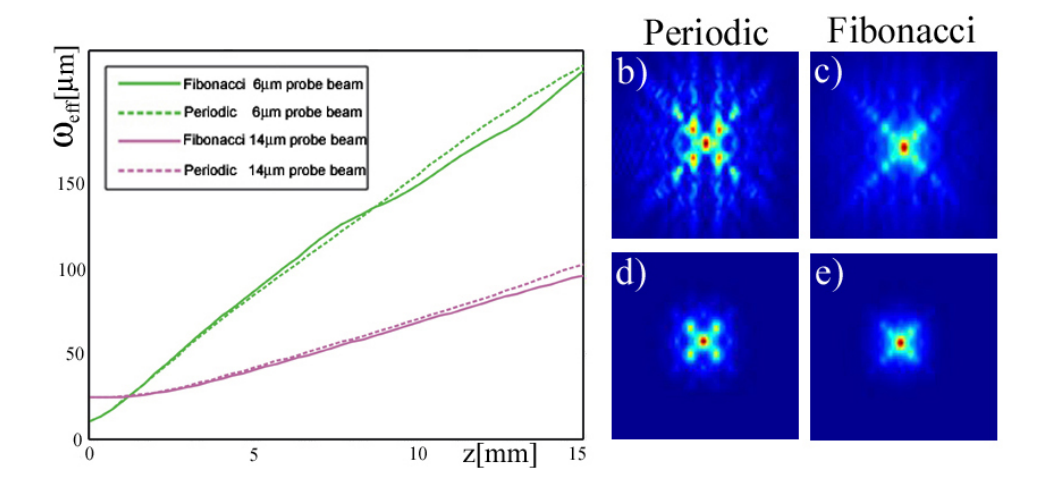


Figure 4. Comparison between localization in periodic and quasiperiodic Fibonacci photonic lattice. (a) Averaged effective beam widths for 2 different values of input probe beam size versus the propagation distance. Intensity distributions at the exit crystal face in periodic lattice for the beam with input size: (b) $6 \mu m$, (d) $14 \mu m$. Averaged intensity beam distribution in Fibonacci lattice for the input beam size: (c) $6 \mu m$, (e) $14 \mu m$.

 $P = \int |E|^4(x,L)dx/\{\int |E|^2(x,L)dx\}^2$ is the inverse participation ratio. We compare beam propagation effects in Fibonacci photonic lattice with appropriate periodic photonic lattice. In our Fibonacci lattice we used periods $\mathcal{A}=42\,\mu\mathrm{m}$ and $\mathcal{B}=26\,\mu\mathrm{m}$. Appropriate periodic photonic lattice is produced in such way that the same number of lattice sites as in quasiperiodic is arranged in periodic manner in the same space (its lattice period in our geometry is $d=32\,\mu\mathrm{m}$).

Figure 4 presents our results with comparison of beam propagation in periodic and quasiperiodic Fibonacci photonic lattices. The averaged effective width (averaged over incident positions) along the propagation distance for Fibonacci lattice is presented for two different input probe beam sizes (6 and 14 µm, cf. Fig. 4(a)), with the effective beam width in appropriate periodic lattices also for two different values of input probe beam size. It should be stressed that the beam width increases slower in Fibonacci lattice as compared to periodic lattices, as the propagation distance is increased. The expansion is just slowed down in Fibonacci lattices. Clearly, the beam propagation in periodic lattice displays the strongest discrete diffraction then in quasiperiodic Fibonacci lattice. For shorter propagation distances (up to 8 mm), beam diffraction in the periodic lattice is slightly less pronounced than in quasiperiodic for input beam size 6 µm. This effect is owing to the weaker coupling between adjacent waveguides in that lattice.

Figure 4 presents also a typical beam spreading at the exit face of the crystal for periodic lattice with $d=32\,\mu\text{m}$, presented after 15 mm of propagation, for input probe beam size 6 μm (b), and 14 μm (d). Averaged intensity distributions, for hundreds different incident positions, in Fibonacci lattice, for both values of input probe beam size, are presented in Fig. 4(c),(e). Comparing with appropriate periodic lattice, a tendency to stronger localization effects in Fibonacci lattice is evident, especially for narrower beam size.

6 Conclusions

In summary, we have observed localization behavior in optically induced Fibonacci photonic lattices. We have analyzed experimentally and numerically propagation and localization characteristics for various incident positions. A very good agreement between experimental and theoretical results is observed. Stronger localization effects were observed in Fibonacci photonic lattice as compared with appropriate periodic photonic lattice. We have investigated influence of different input probe beam size on the localization effects in Fibonacci waveguide arrays. More pronounced localization is observed in the case of narrow probe beam. We believe our results can be generalized to other kinds of quasiperiodic optically induced lattices, using the presented ideas and methods.

Acknowledgments

This work is supported by the German Academic Exchange Service (Project 56267010) and Ministry of Education, Science and Technological Development, Republic of Serbia (Project OI 171036).

References

- [1] D. Shechtman, I. Blech, D. Gratias, and J. W. Cahn, "Metallic Phase with Long-Range Orientational Order and No Translational Symmetry," Phys. Rev. Lett. **53**, 1951 (1984).
- [2] D. Levine and P. J. Steinhardt, "Quasicrystals: A New Class of Ordered Structures," Phys. Rev. Lett. **53**, 2477 (1984).
- [3] M. Kohmoto, B. Sutherland, and K. Iguchi, "Localization in Optics: Quasiperiodic Media," Phys. Rev. Lett. **58**, 2436 (1987).
- [4] W. Steurer and D. Sutter-Widmer, "Photonic and phononic quasicrystals," J. Phys. D 40, R229 (2007).
- [5] Z. V. Vardeny, A. Nahata and A. Agrawal, "Optics of photonic quasicrystals," Nat. Photon. 7, 177 (2013).
- [6] G. Gumbs and M. K. Ali, "Dynamical Maps, Cantor Spectra, and Localization for Fibonacci and Related Quasiperiodic Lattices," Phys. Rev. Lett. 60, 1081 (1988).
- [7] W. Gellermann, M. Kohmoto, B. Sutherland, and P. C. Taylor, "Localization of Light Waves in Fibonacci Dielectric Multilayers," Phys. Rev. Lett. **72**, 633 (1994).
- [8] L. DalNegro, C. J. Oton, Z. Gaburro, L. Pavesi, P. Johnson, A. Lagendijk, R. Righini, M. Colocci, and D. S. Wiersma, "Light Transport through the Band-Edge States of Fibonacci Quasicrystals," Phys. Rev. Lett. 90, 055501 (2003).
- [9] E. L. Albuquerque and M. G. Cottam, "Theory of elementary excitations in quasiperiodic structures," Phys. Rep. **376**, 225 (2003).

- [10] Y. Lahini, R. Pugatch, F. Pozzi, M. Sorel, R. Morandotti, N. Davidson, and Y. Silberberg, "Observation of a Localization Transition in Quasiperiodic Photonic Lattices," Phys. Rev. Lett. 103, 013901 (2009).
- [11] K. Vynck, M. Burresi, F. Riboli, and D. S. Wiersma, "Photon management in two-dimensional disordered media," Nat. Mater. 11, 1017 (2012).
- [12] E. R. Martins, J. Li, Y. K. Liu, V. Depauw, Z. Chen, J. Zhou, and T. F. Krauss, "Deterministic quasi-random nanostructures for photon control," Nat. Commun. 4, 2665 (2013).
- [13] F. Diebel, P. Rose, M. Boguslawski, and C. Denz, "Optical induction scheme for assembling nondiffracting aperiodic Vogel spirals," Appl. Phys. Lett **104**, 191101 (2014).
- [14] F. Diebel, D. Leykam, M. Boguslawski, P. Rose, C. Denz, and A. S. Desyatnikov, "All-optical switching in optically induced nonlinear waveguide couplers," Appl. Phys. Lett 104, 261111 (2014).
- [15] P. Rose, M. Boguslawski, and C. Denz, "Nonlinear lattice structures based on families of complex nondiffracting beams," New J. Phys. 14, 33018 (2012).